



# Performance of a highly reactive impregnated $\text{Fe}_2\text{O}_3/\text{Al}_2\text{O}_3$ oxygen carrier with $\text{CH}_4$ and $\text{H}_2\text{S}$ in a 500 $\text{W}_{\text{th}}$ CLC unit



A. Cabello, C. Dueso, F. García-Labiano, P. Gayán\*, A. Abad, L.F. de Diego, J. Adánez

*Instituto de Carboquímica (ICB-CSIC), Department of Energy and Environment, Miguel Luesma Castán 4, Zaragoza 50018, Spain*

## HIGHLIGHTS

- The effect of  $\text{H}_2\text{S}$  on the CLC process using a Fe-based oxygen carrier was analyzed.
- The presence of  $\text{H}_2\text{S}$  hardly affected the reactivity and the combustion efficiency.
- All the sulfur fed was released as  $\text{SO}_2$  in the flue gas from the FR.
- No sulfur was detected in the oxygen carrier particles.
- This impregnated Fe-based oxygen carrier was highly reactive and sulfur resistant.

## ARTICLE INFO

### Article history:

Received 19 September 2013

Received in revised form 10 December 2013

Accepted 11 December 2013

Available online 22 December 2013

### Keywords:

$\text{CO}_2$  capture

Chemical-looping combustion

Iron

Oxygen carrier

Hydrogen sulfide

## ABSTRACT

A synthetic Fe-based oxygen carrier prepared by impregnation using  $\gamma\text{-Al}_2\text{O}_3$  as support, successfully tested for gas CLC combustion, has been now evaluated with respect to gas combustion in a 500  $\text{W}_{\text{th}}$  CLC continuous unit when the fuel,  $\text{CH}_4$ , contained variable amounts of  $\text{H}_2\text{S}$ .

Full gas combustion was reached at oxygen carrier-to-fuel ratio values higher than 1.5. The presence of sulfur in the fuel gas hardly affected the reactivity and combustion efficiency of the oxygen carrier, independently of the amount of sulfur in the gas stream. All the sulfur introduced as  $\text{H}_2\text{S}$  in the fuel reactor (FR) was released in the same reactor as  $\text{SO}_2$ . Furthermore, oxygen carrier particles extracted from the CLC unit after the experimental tests with  $\text{H}_2\text{S}$  addition were characterized by means of different techniques and no sulfur was detected in any case. The impregnated Fe-based oxygen carrier was highly reactive and sulfur resistant, and can be considered as a suitable material for CLC with gaseous fuels that contain sulfur.

© 2013 Elsevier Ltd. All rights reserved.

## 1. Introduction

Chemical Looping Combustion (CLC) is a combustion technology where an oxygen carrier, usually a metal oxide, is used to transfer oxygen from the combustion air to the fuel, thus avoiding direct contact between air and fuel [1,2]. This technology has the advantage that  $\text{CO}_2$  is inherently separated, thus there is no energy loss in the separation and no costs associated with gas separation equipment and operation. The solid circulates between two interconnected reactors, the fuel (FR) and the air reactor (AR). In the FR, the metal oxide reacts with the gaseous fuel to produce  $\text{CO}_2$  and  $\text{H}_2\text{O}$ . A high concentrated  $\text{CO}_2$  stream, ready for compression and sequestration, can be obtained condensing the steam. The oxygen carrier is oxidized again in the AR so that it is ready to start a new cycle.

In the last years, different metal oxide systems have been proposed to be used as oxygen carriers in the CLC process [2]. Among them, Fe-based oxygen carriers present several advantages such as adequate crushing strength values and a low trend towards carbon formation. Other non-physical-chemical aspects, such as the cost of the oxygen carrier, the availability or its friendly environmental behavior are also advantageous with respect to other metal oxides used for the CLC process.

Iron compounds can present different final oxidation states during reduction reaction ( $\text{Fe}_2\text{O}_3$ ,  $\text{Fe}_3\text{O}_4$ ,  $\text{FeO}$  and  $\text{Fe}$ ). The reducing gas composition and temperature are the variables that determine the stable Fe species. For an industrial CLC system, only the transformation from hematite to magnetite ( $\text{Fe}_2\text{O}_3\text{--Fe}_3\text{O}_4$ ) is applicable due to thermodynamic limitations [2]. If the iron oxide is further reduced to wustite ( $\text{FeO}$ ) or  $\text{Fe}$ , the  $\text{CO}_2$  purity obtained in the FR decreased considerably since the  $\text{CO}$  and  $\text{H}_2$  concentrations in equilibrium increase in a great extent [3]. However, when alumina or titania is present in the oxygen carrier particles, reduced compounds such as  $\text{FeO}\cdot\text{Al}_2\text{O}_3$  or  $\text{FeO}\cdot\text{TiO}_2$  can be formed allowing full

\* Corresponding author. Tel.: +34 976 733 977; fax: +34 976 733 318.

E-mail address: [pgayan@icb.csic.es](mailto:pgayan@icb.csic.es) (P. Gayán).

combustion of the fuel to  $\text{CO}_2$  and  $\text{H}_2\text{O}$ . In these conditions, a further reduction of the iron compounds is achieved in comparison with the  $\text{Fe}_2\text{O}_3/\text{Fe}_3\text{O}_4$  system [4,5].

Up to now, several natural or synthetic Fe-based oxygen carriers have been tested at lab scale (TGA and fluidized bed reactors) and small continuous CLC units for gaseous fuels [6–13]. In general, Fe-based oxygen carriers present weak redox characteristics and low combustion conversions when  $\text{CH}_4$  is used as fuel. Nevertheless, our research group at the Instituto de Carboquímica (ICB-CSIC) developed a highly reactive Fe-based oxygen carrier prepared by the incipient hot impregnation method using  $\text{Al}_2\text{O}_3$  as support [13]. Complete combustion efficiencies were reached at low oxygen carrier-to-fuel ratio ( $\phi$ ) values when the temperature in the FR was 1153 K. The corresponding solids inventory in the FR was around 500 kg/MW<sub>th</sub>, which corresponds to a Fe inventory of 50 kg/MW<sub>th</sub>. These values are the lowest referred in the literature for any kind of Fe-based oxygen carrier, both natural or synthetic.

A required step for the development of an optimum oxygen carrier for the CLC process is the evaluation of its behavior in similar conditions to the ones present at industrial scale. All the previous works with Fe-based oxygen carriers have been carried out using methane, CO, or/and  $\text{H}_2$  to simulate the composition of natural gas, syngas or PSA-off gas. However, real fuel gases at industrial scale can contain variable amounts of sulfur compounds, such as  $\text{H}_2\text{S}$  and COS. Very small amounts of  $\text{H}_2\text{S}$  (~20 vppm) are present in natural gas [14]. In the case of a refinery fuel gas, the  $\text{H}_2\text{S}$  content varied depending on the site, and concentrations up to 800 vppm can be obtained. Finally, this value can be as high as 8000 vppm for raw syngas generated from coal gasification [15].

The presence of sulfur compounds can have a great influence over the design of an industrial CLC plant. Environmentally, the legislation about gaseous emissions must be fulfilled so that the sulfur released as  $\text{SO}_2$  in the AR gas outlet stream should be lower than the legal limit value. Furthermore, sulfur can also be emitted in the FR gas outlet stream affecting in this case the quality of the  $\text{CO}_2$  produced [16,17].

From an operational point of view, the oxygen carrier can be poisoned by the sulfur compounds formed from the reaction between the metal oxide and sulfurous gases such as  $\text{H}_2\text{S}$ . The damage to the material can be revealed in terms of reactivity, transport capacity and combustion efficiency reduction. Formation of solid sulfur compounds depends on sulfur compound concentrations as well as temperature and pressure [3].

Thermodynamic calculations about the fate of  $\text{H}_2\text{S}$  in a CLC process have been previously conducted taking into account different metal oxides as oxygen carriers, operating conditions (temperature, pressure, and  $\text{H}_2\text{S}$  concentrations) and gaseous fuels ( $\text{CH}_4$ , CO or  $\text{H}_2$ ). Jerndal et al. [3] and Wang et al. [18] concluded that there was no risk of iron sulfide or iron sulfate formation under usual CLC process conditions in terms of temperature, concentration of sulfur-containing gases or oxygen excess. However, previous works in our research group [19,20] found that the fate of sulfur in a CLC process could not be predicted based only with thermodynamic analyses. The thermodynamic calculations carried out by García-Labiano et al. [19] regarding the effect of sulfur on Ni-based oxygen carriers predicted the absence of nickel sulfides formation at some operating conditions. However, experimental data showed that the formation of sulfides in the fuel reactor was evident even in those operating conditions selected to avoid sulfides formation according to thermodynamics. This fact was explained according to the different gas atmosphere existing in the lower zone of the fuel reactor, which was a fluidized bed. Furthermore, Forero et al. [20] stated that, according to a thermodynamic study, the formation of copper sulfides should be avoided at oxygen carrier-to-fuel ratios ( $\phi$ ) above 1. Nevertheless, the presence of  $\text{CH}_4$  and low concentrations of  $\text{CO}_2$  and  $\text{H}_2\text{O}$  in the fuel reactor favored

the formation of copper sulfides and the deactivation of the Cu-based oxygen carrier at  $\phi = 1.3$ . Moreover, other factors like kinetics of sulfur compounds can affect the sulfur gas product distribution in the CLC system predicted by thermodynamics. Finally, it is important to note that the conclusions found by Jerndal et al. [3] and Wang et al. [18] were obtained considering the pair  $\text{Fe}_2\text{O}_3/\text{Fe}_3\text{O}_4$  as Fe-species. In this work, alumina is used as support and hence results can be different since  $\text{FeO-Al}_2\text{O}_3$  specie can appear as Fe-reduced compound instead of  $\text{Fe}_3\text{O}_4$ .

Up to now, the effect of sulfur on the performance of Fe-based oxygen carriers in continuous CLC units has not been studied yet. In this sense, more tests in continuous facilities are needed to gain an adequate understanding of the behavior and usefulness of these particles for this kind of combustion technology. The aim of this work was to test the performance of a highly reactive synthetic Fe-based oxygen carrier when the fuel,  $\text{CH}_4$ , contained variable amounts of  $\text{H}_2\text{S}$  (up to 2000 ppm). The influence of  $\text{H}_2\text{S}$  concentration on the gas products distribution and combustion efficiency, sulfur splitting between FR and AR and oxygen carrier deactivation were investigated under continuous operation in a 500 W<sub>th</sub> CLC prototype. Moreover, the evolution of the oxygen carrier properties and its behavior during long-term operation was also analyzed.

## 2. Experimental section

### 2.1. Oxygen carrier material

A synthetic Fe-based oxygen carrier prepared by impregnation,  $\text{Fe}_2\text{O}_3/\text{Al}_2\text{O}_3$  oxygen carrier, has been used in this work. Commercial  $\gamma\text{-Al}_2\text{O}_3$  (Puralox NWA-155, Sasol Germany GmbH) particles of 0.1–0.32 mm, with density of 1.3 g/cm<sup>3</sup> and porosity of 55.4% were selected as support. The oxygen carrier was prepared impregnating the support heated at 353 K in a planetary mixer with a saturated iron nitrate solution [ $\text{Fe}(\text{NO}_3)_3 \cdot 9\text{H}_2\text{O}$ ] at 333–353 K (3.8 M). The volume of solution added corresponded to the total pore volume of the support particles. This solution was slowly added to the alumina particles with thorough stirring at hot temperature (353 K). The material resulting from the first impregnation was calcined at 823 K in air atmosphere for 30 min to decompose the impregnated metal nitrate into the metal oxide. Finally, after the second impregnation, the oxygen carrier was sintered in a furnace at 1223 K for 1 h. The main physical and chemical properties of this oxygen carrier can be found in Gayán et al. [13].

### 2.2. Oxygen carrier characterization

Several techniques have been used to physically and chemically characterize both fresh and after-used oxygen carrier particles. The reactivity of the particles was determined by TGA. The force needed to fracture a particle was determined using a Shimpo FGN – 5X crushing strength apparatus. The crushing strength was obtained as the average value of at least 20 measurements. The attrition resistance was determined using a three-hole air jet attrition tester, ATT-100M, configured according to ASTM-D-5757-95 [21]. As specified in the ASTM method, 50 g of material, in this case fresh and used samples, were tested under 10 L/min of air flow. The weight loss of fines was recorded at 1 h and 5 h of time on stream, respectively. The percentage of fines after a 5 h test is the Air Jet Attrition Index (AJI). According to the ASTM method, particles with a size lower than 20  $\mu\text{m}$  are considered as fines. The identification of crystalline chemical species was carried out by powder X-ray Diffraction (XRD) in a Bruker AXS D8 Advance, equipped with monochromatic beam diffracted graphite, using Ni-filtered “Cu K $\alpha$ ” radiation. On the other hand, the reducibility of the oxygen carrier particles was determined by temperature-programmed reduction (TPR) experiments in a flow

apparatus AUTOCHEM II from Micromeritics. Finally, the oxygen carrier particles were also analyzed in a scanning electron microscope (SEM) ISI DS-130 coupled to an ultra thin window PGT Prism detector for energy-dispersive X-ray (EDX) analysis in order to determine the microstructure and to carry out an elemental microanalysis.

### 2.3. Reactivity of the oxygen carrier

Reactivity tests of fresh and after-used particles were carried out in a TGA, CI electronics type, described elsewhere [22]. The reactivity of the oxygen carrier was determined with  $\text{CH}_4$  as reducing gas. All the reactivity tests were carried out at 1223 K and at atmospheric pressure. The gas composition was 15 vol.%  $\text{CH}_4$ , and 20 vol.%  $\text{H}_2\text{O}$  was added to avoid carbon formation by  $\text{CH}_4$  decomposition during reduction reaction. Finally, nitrogen was used to balance. For oxidation reaction, pure air was used as reacting gas. After weight stabilization, the experiment was started by exposing the oxygen carrier to three alternating reducing and oxidizing cycles.

The conversion of solids for the reduction reaction was calculated as:

$$X_r = \frac{m_{\text{ox}} - m}{R_{\text{OC}} \cdot m_{\text{ox}}} \quad (1)$$

$m_{\text{ox}}$  being the mass of the fully oxidized solids,  $m$  the instantaneous mass of the sample and  $R_{\text{OC}}$  the oxygen transport capacity for the transformation between  $\text{Fe}_2\text{O}_3$  and  $\text{FeO} \cdot \text{Al}_2\text{O}_3$ . The conversion of the oxidation reaction was calculated as  $X_o = 1 - X_r$ .

### 2.4. ICB-CSIC-g1. facility

A schematic diagram of the 500  $\text{W}_{\text{th}}$  chemical-looping combustion prototype used for the experimental tests is shown in Fig. 1. This facility was composed of two interconnected fluidized-bed reactors, a riser for solid transport, a solid valve to control the solids fed to the FR, a loop seal and a cyclone. This design allowed the variation and control of the solid circulation flow rate between both reactors.

The FR (1) and the AR (3) are two bubbling fluidized-beds (0.05 m i.d.) with a bed height of 0.1 m. The AR was followed by a riser (4) of 0.02 m i.d. and 1 m height. A further description of this CLC prototype is present elsewhere [19,20].

To study the effect of sulfur on the oxygen carrier, the CLC pilot plant included two mass flow controllers for  $\text{H}_2\text{S}$  and  $\text{H}_2$ . Small amounts of  $\text{H}_2$  (up to 1 vol.%) were fed together with  $\text{H}_2\text{S}$  to avoid the decomposition of  $\text{H}_2\text{S}$  in the feeding lines. Furthermore, the gas lines downstream the FR were heated by electrical resistances in order to avoid steam condensation and  $\text{H}_2\text{SO}_4$  formation. A nondispersive infrared (NDIR) analyzer (Siemens Ultramat U22) was used to detect the  $\text{SO}_2$  concentrations obtained at the AR gas outlet stream. To analyze the FR gas outlet stream, a gas chromatograph (Varian 3400-CX GC) equipped with a PORAPAK-Q packed column for chromatographic separation and a sulfur-specific flame photometric detector (FPD) was used. In this way, it was possible the detection of the different gaseous sulfur compounds that could appear in the FR as  $\text{H}_2\text{S}$ ,  $\text{SO}_2$ ,  $\text{COS}$ ,  $\text{CS}_2$ , etc. The chromatograph was calibrated in the range of 0–1500 vppm for  $\text{H}_2\text{S}$  and 0–2000 vppm for  $\text{SO}_2$ .

### 2.5. Testing conditions

The total solids inventory in the system was 1.2 kg approximately, of which 0.3 and 0.5 kg were in the FR and AR, respectively. A total operation time of 75 h at hot conditions, 50 of them were with sulfur addition, was carried out using the same batch of

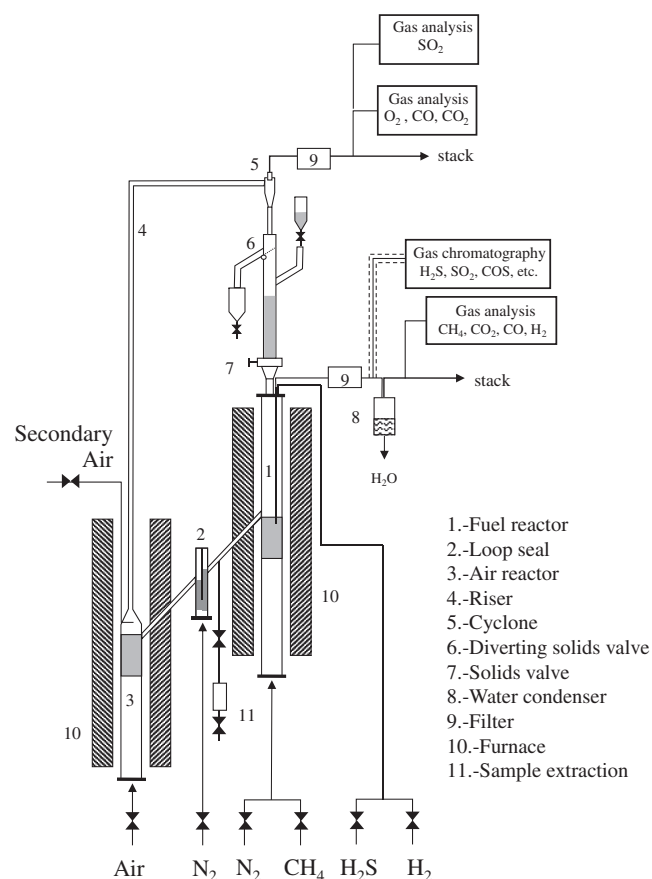


Fig. 1. Schematic diagram of the ICB-CSIC-g1 facility.

oxygen carrier particles. The temperatures in the AR and FR were always kept constant at about 1223 K and 1173 K respectively. The inlet gas flow in the FR was 170  $\text{L}_\text{N}/\text{h}$  (0.1 m/s) for all the tests. Air was used as fluidizing gas in the AR, which was divided into the primary air, added from the bottom bed (720  $\text{L}_\text{N}/\text{h}$ ), and the secondary air, added at the top of the bubbling bed to help particle entrainment in the riser (150  $\text{L}_\text{N}/\text{h}$ ). Nitrogen was also used to fluidize the bottom loop seal (37.5  $\text{L}_\text{N}/\text{h}$ ).

The fuel gas was a stream containing  $\text{CH}_4$ , different amounts of  $\text{H}_2\text{S}$  and  $\text{N}_2$  to balance.  $\text{H}_2\text{S}$  concentrations used in the different tests (750, 1300 and 2000 vppm) were calculated with respect to the total inlet gas flow in the FR, i.e., 170  $\text{L}_\text{N}/\text{h}$ . Three different experimental tests series were carried out within the scope of this work. Table 1 shows a summary of the main variables used in each test. Combustion test 1 is a reference test without sulfur addition. In tests 2–4, it was determined the effect of the  $\text{H}_2\text{S}$  content on the behavior of the Fe-based material working at high oxygen carrier-to-fuel ratios ( $\phi = 1.9$ ). Finally, tests 5–9 were carried out at low oxygen carrier-to-fuel ratios ( $\phi < 1.4$ ) using two different  $\text{H}_2\text{S}$  concentrations to analyze the effect of sulfur when  $\text{CH}_4$  was not completely converted.

The oxygen carrier-to-fuel ratio ( $\phi$ ) was defined by Eq. (2), as:

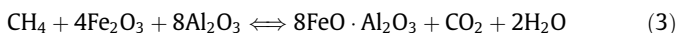
$$\phi = \frac{F_{\text{Fe}_2\text{O}_3}}{4 \cdot F_{\text{CH}_4}} \quad (2)$$

where  $F_{\text{Fe}_2\text{O}_3}$  is the molar flow rate of  $\text{Fe}_2\text{O}_3$  and  $F_{\text{CH}_4}$  is the inlet molar flow rate of  $\text{CH}_4$  in the FR. This parameter can be defined as the ratio between the oxygen supplied and the oxygen needed to stoichiometrically react with the fuel flow. As the  $\text{H}_2\text{S}$  and  $\text{H}_2$  concentrations are practically negligible in relation to the  $\text{CH}_4$  concentration fed to the CLC system, it can be considered that a

**Table 1**  
Operating conditions used during experiments with H<sub>2</sub>S in the CLC facility.

Test	CH <sub>4</sub> conc. (vol.%)	H <sub>2</sub> S in (vppm)	F <sub>2</sub> (kg/h)	φ	Power (W <sub>th</sub> )	Accumulated combustion time (h)
1	30	0	16	1.9	507	4
2	30	2000	16	1.9	507	10
3	30	1300	16	1.9	507	18
4	30	750	16	1.9	507	20
5	30	1300	12.0	1.4	507	26
6	30	1300	9.4	1.1	507	34
7	30	1300	8.5	1.0	507	42
8	30	2000	11.2	1.3	507	48
9	30	2000	10.3	1.2	507	54

value of  $\phi = 1$  corresponds to the stoichiometric relation between Fe<sub>2</sub>O<sub>3</sub> and CH<sub>4</sub> in reaction (3).



In reaction (3) iron aluminate (FeO·Al<sub>2</sub>O<sub>3</sub>) is the Fe-reduced compound allowing complete combustion of the gaseous fuel to CO<sub>2</sub> and H<sub>2</sub>O. In this sense, when hematite, Fe<sub>2</sub>O<sub>3</sub>, is supported over alumina particles, the oxygen transport capacity of the oxygen carrier is increased by three times in comparison with the transformation from hematite to magnetite (Fe<sub>2</sub>O<sub>3</sub>–Fe<sub>3</sub>O<sub>4</sub>) [13].

The combustion efficiency ( $\eta_c$ ) has been defined as the ratio of oxygen consumed by the gas leaving the FR to that consumed by the gas when the fuel is completely burnt to CO<sub>2</sub> and H<sub>2</sub>O. So, the  $\eta_c$  gives an idea about how the CLC operation is close or far from the complete combustion of the fuel, i.e.,  $\eta_c = 100\%$ .

$$\eta_c = \frac{(2x_{\text{CO}_2} + x_{\text{CO}} + x_{\text{H}_2\text{O}})_{\text{out}} \cdot F_{\text{out}}}{(4x_{\text{CH}_4})_{\text{in}} \cdot F_{\text{in}}} \cdot 100 \quad (4)$$

where  $F_{\text{in}}$  is the molar flow of the inlet gas stream,  $F_{\text{out}}$  is the molar flow of the outlet gas stream, and  $x_i$  is the molar fraction of the gas  $i$ . It must be considered that the H<sub>2</sub>S combustion process had a very small relevance in the  $\eta_c$  values since the amount of H<sub>2</sub>S fed was very low in relation to CH<sub>4</sub>.

### 3. Results

#### 3.1. Thermodynamic calculations

Several thermodynamic studies regarding the fate of sulfur with Fe-based oxygen carriers have been previously carried out [3,18]. These thermodynamic studies were conducted without taking into account the formation of FeO·Al<sub>2</sub>O<sub>3</sub> as a reduced iron phase when alumina is used as support.

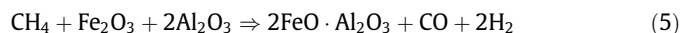
Therefore, a thermodynamic study was now carried out using the HSC Chemistry 6.1 [23] software to determine the fate of sulfur when a Fe<sub>2</sub>O<sub>3</sub>/Al<sub>2</sub>O<sub>3</sub> oxygen carrier was used. This program finds the most stable phase combination and seeks the phase composition where the Gibbs energy of the system reaches its minimum at a fixed mass balance, constant pressure and temperature.

The calculations were conducted considering CH<sub>4</sub> as fuel, H<sub>2</sub>S concentrations up to 5000 vppm and operating temperatures from 973 K to 1273 K. Fig. 2 shows the thermodynamic equilibrium of the compounds existing in the FR at 1173 K as a function of the oxygen present in this reactor, that is, as a function of the oxygen carrier-to-fuel ratio,  $\phi$ . The values were expressed as the volumetric percentage of gas composition for methane combustion and the mass percentage of sulfur species present in the products in relation to the methane and sulfur fed into the system, respectively. Regarding the equilibrium gas composition, it can be observed that at  $\phi$  values above 1, complete combustion of CH<sub>4</sub> to CO<sub>2</sub> and H<sub>2</sub>O

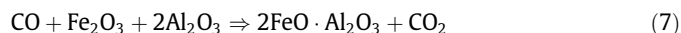
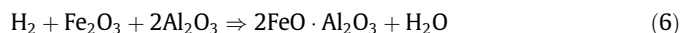
was achieved. In these conditions, Fe<sub>2</sub>O<sub>3</sub> and FeO·Al<sub>2</sub>O<sub>3</sub> were the only iron species present. If the parameter  $\phi$  was decreased below 1, unreacted H<sub>2</sub> and CO appeared reaching their maximum values when the equilibrium Fe–FeO·Al<sub>2</sub>O<sub>3</sub> was found. In that case, CO<sub>2</sub> and H<sub>2</sub>O were not present in the gas equilibrium and CH<sub>4</sub> appeared as an unreacted gas. The CH<sub>4</sub> concentration at equilibrium increased at very low  $\phi$  values when hematite was fully reduced to metallic iron. Regarding the sulfur species present in the thermodynamic equilibrium, the unique stable sulfur compound in the FR was SO<sub>2</sub> when  $\phi \geq 1$ . At sub-stoichiometric conditions, different solid and gaseous sulfur species can appear depending on the amount of oxygen present in the system. Only working at very low oxygen carrier-to-fuel ratios ( $\phi < 0.1$ ), a stable solid sulfur compound, Fe<sub>0.877</sub>S, could be formed when elemental Fe exists. The thermodynamic calculations made at different temperatures and H<sub>2</sub>S concentrations showed similar results.

In order to understand in a better way the results shown in Fig. 2, a compilation of all the possible reactions regarding a Fe-based oxygen carrier that reacts with CH<sub>4</sub> and H<sub>2</sub>S is shown, both in the FR and AR.

Using CH<sub>4</sub> as gaseous fuel and Fe<sub>2</sub>O<sub>3</sub> impregnated over Al<sub>2</sub>O<sub>3</sub> as oxygen carrier, the overall reaction in the FR is given by Eq. (3). CO and H<sub>2</sub> can appear by partial oxidation reaction between CH<sub>4</sub> and the Fe-based oxygen carrier.



Both compounds can later react with the oxygen carrier by the following ways:



When the fuel gas contains H<sub>2</sub>S, the number of chemical reactions that can be carried out in the FR increases. At  $\phi$  values above 1, the main reaction that takes place is the one that involves the iron oxide with the H<sub>2</sub>S in order to form SO<sub>2</sub> through equation (8).

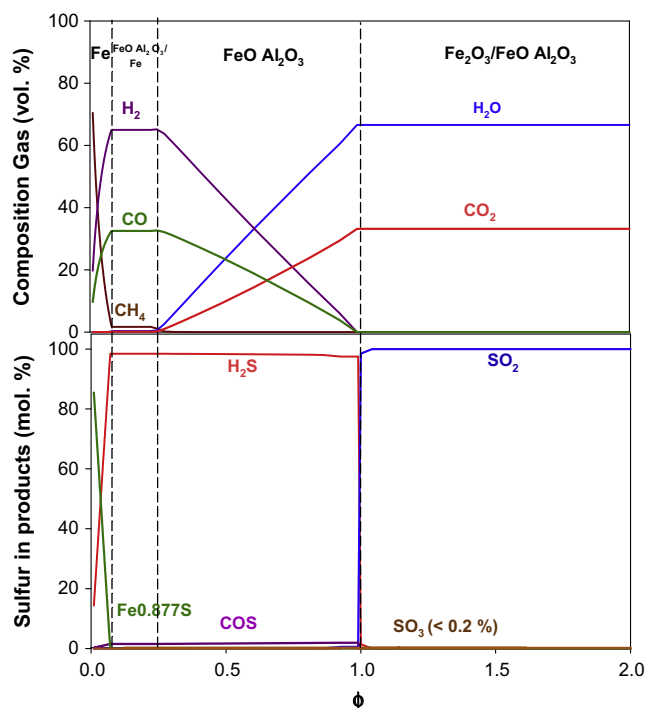
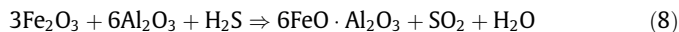


**Fig. 2.** Thermodynamic equilibrium as a function of parameter  $\phi$ . Fuel gas: CH<sub>4</sub>; H<sub>2</sub>S: 5000 vppm;  $T_{\text{FR}} = 1173$  K.

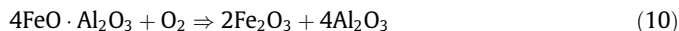




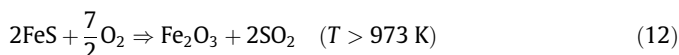
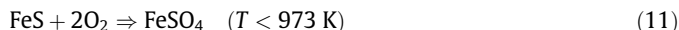
Thermodynamic calculations showed that  $\text{Fe}_{0.877}\text{S}$  was the only stable iron sulfide that could be formed when elemental Fe exists in the equilibrium.



The reduced oxygen carrier particles are transported to the AR where the following reactions can take place. Firstly, the iron aluminate is oxidized to hematite:



Furthermore, the iron sulfide that comes from the FR can react with the oxygen added in the AR to  $\text{FeSO}_4$  or  $\text{Fe}_2\text{O}_3$  with  $\text{SO}_2$  release.



As the temperature in the AR of a CLC unit is always higher than 973 K, it would be supposed that the iron sulfide would be released in this reactor in form of  $\text{SO}_2$ .

### 3.2. Effect of $\text{H}_2\text{S}$ on the combustion efficiency

To determine the behavior of the oxygen carrier in atmospheres that contain sulfur, several tests were carried out in the 500 W<sub>th</sub> CLC prototype under continuous operating conditions using a mixture of  $\text{CH}_4$  and  $\text{H}_2\text{S}$  as fuel gas. Reactivity, combustion efficiency, agglomeration, and sulfur splitting between reactors were analyzed. As it was previously mentioned, concentrations up to 2000 vppm of  $\text{H}_2\text{S}$  were used in the fuel stream fed to the FR.

Fig. 3 summarizes the main results obtained during the experimental work showing the gas concentration of the different compounds measured at the outlet streams of the FR and AR. In this Figure, tests 1–4 with high oxygen carrier-to-fuel ratio values ( $\phi = 1.9$ ) are presented. The combustion of the  $\text{CH}_4$  was complete to  $\text{CO}_2$  and  $\text{H}_2\text{O}$ . Furthermore, it was also observed that the gas concentration profiles were not affected by the presence of  $\text{H}_2\text{S}$  in the system independently of the  $\text{H}_2\text{S}$  concentration introduced. As it was predicted from the thermodynamic calculations, all the sulfur introduced as  $\text{H}_2\text{S}$  in the FR was oxidized to  $\text{SO}_2$ .  $\text{H}_2\text{S}$ , COS and  $\text{CS}_2$  were not detected in any case at the outlet of the FR. The concentrations of  $\text{CO}_2$  and  $\text{SO}_2$  measured in dry basis in the FR were a bit lower than the  $\text{CH}_4$  and  $\text{H}_2\text{S}$  concentrations fed into the system due to the small dilution produced by the  $\text{N}_2$  flowing from the loop seal into the FR. Moreover, neither  $\text{CO}_2$  nor CO was detected in the AR gas stream, which indicated the absence of gas leakage between reactors and no carbon formation in the FR. Finally, it is important to highlight that  $\text{SO}_2$  was never detected at the outlet of the AR. The operation of the prototype was very stable for a long period of time even in those cases where high amounts of  $\text{H}_2\text{S}$  were added (1300 and 2000 vppm).

In tests 5–9, at which the oxygen carrier-to-fuel ratios were close to stoichiometry conditions,  $\text{CO}_2$  concentration was lower than that corresponding to full fuel combustion and some unconverted  $\text{CH}_4$  appeared while CO and  $\text{H}_2$  concentrations were very low in all cases (<0.2 vol.%). It must be pointed out that a  $\phi$  value higher than 1.5 at 1153 K was determined in a previous work [13] to obtain full combustion of  $\text{CH}_4$  in this facility with the oxygen carrier material. The addition of different amounts of  $\text{H}_2\text{S}$  to the gaseous fuel stream caused a negligible effect on the  $\text{CO}_2$  and  $\text{CH}_4$  concentrations at the outlet stream from the FR.

The combustion efficiency,  $\eta_c$ , reached in the CLC unit was used as comparison parameter to evaluate the behavior of the oxygen carrier during the different tests carried out. Fig. 4 shows the effect

of the oxygen carrier-to-fuel ratio on the combustion efficiency for each test. As it can be observed, there were no significant differences with respect to the results obtained by Gayán et al. [13] working with the same oxygen carrier in the absence of  $\text{H}_2\text{S}$ . In this sense, it can be concluded that the presence of  $\text{H}_2\text{S}$  in the fuel gas (tests 2–9) hardly affected the combustion efficiency, independently of the amount of sulfur present in the fuel stream.

Regarding the oxygen carrier-to-fuel ratio value needed to obtain full fuel combustion, it can be stated that a  $\phi$  value of 1.5 is a low value that permits to fulfill the mass and energy balances in the CLC system. Furthermore, this oxygen carrier-to-fuel ratio value is similar to those found for other Cu- and Ni-based oxygen carriers for  $\text{CH}_4$  combustion [24,25].

Sulfur mass balances made in the CLC system at the different tests are summarized in Table 2. These balances were carried out by integration the  $\text{SO}_2$  concentration present at the gas outlet stream of the FR since the emission of unreacted  $\text{H}_2\text{S}$  in the FR or  $\text{SO}_2$  in the AR was never detected in any test. Furthermore, although  $\text{SO}_3$  could not be measured continuously, thermodynamic analyses carried out at usual CLC operating conditions demonstrated that the presence of  $\text{SO}_3$  was almost negligible in the FR, and for that reason the influence of this compound on the sulfur mass balances was not considered. Sulfur balances closed in a range of  $\pm 5$  wt.% in all cases, which can be attributed to experimental errors, indicating the absence of a noteworthy iron sulfides formation in the FR. However, a deeply characterization of used oxygen carrier particles extracted from the CLC unit was made in order to corroborate these results.

Finally, it can be highlighted that a smooth operation of the CLC unit was achieved during the 75 h of experimental work, and operational problems, such as corrosion, were never found due to the presence of  $\text{H}_2\text{S}$  in the CLC plant.

### 3.3. Characterization of the oxygen carrier

#### 3.3.1. Mechanical integrity and tendency for agglomeration

The mechanical integrity of the fresh and used material was evaluated by different methods. First, the crushing strength of the fresh particles was measured in a dynamometer as 1.5 N. This value dropped up to 0.9 N for oxygen carrier particles taken out from the CLC unit after 75 h of operation. This value is lower to the one reported by Gayán et al. [13] due to a longer operation time (75 h vs 46 h). Also, the attrition index of the fresh particles was determined by the ASTM-D-5757–95 method as 4.7%. Materials with AIJ values below 5% are generally considered suitable for use in a transport reactor in the catalyst industry [26]. However, this value increased up to 12.8% for the particles extracted from the CLC unit at the end of the experimental work. This increase can be due to the drop of the crushing strength that the particles underwent during its long-term operation inside the CLC unit.

Moreover, an attrition rate was experimentally determined during the CLC process. Particles elutriated from both reactors were recovered in the cyclones and filters and weighted to calculate the attrition rate. Those particles whose size was lower than 40  $\mu\text{m}$  were considered as attrited particles. The attrition rate measured of the  $\text{Fe}_2\text{O}_3/\text{Al}_2\text{O}_3$  oxygen carrier during these experimental tests was similar to the one obtained by Gayán et al. [13] with the same Fe-based oxygen carrier but without  $\text{H}_2\text{S}$  addition. In both cases, the attrition rate was high during the first hours as a consequence of the rounding effects on the irregularities of the particles and because of the fines stuck to the particles during the preparation. Finally, the attrition rate of the  $\text{Fe}_2\text{O}_3/\text{Al}_2\text{O}_3$  oxygen carrier was stabilized at approximately 0.09 wt.%/h, giving a particle lifetime of 1100 h.

Finally, it is important to point out that during the 75 h of operation at hot conditions in the CLC unit, the oxygen carrier particles

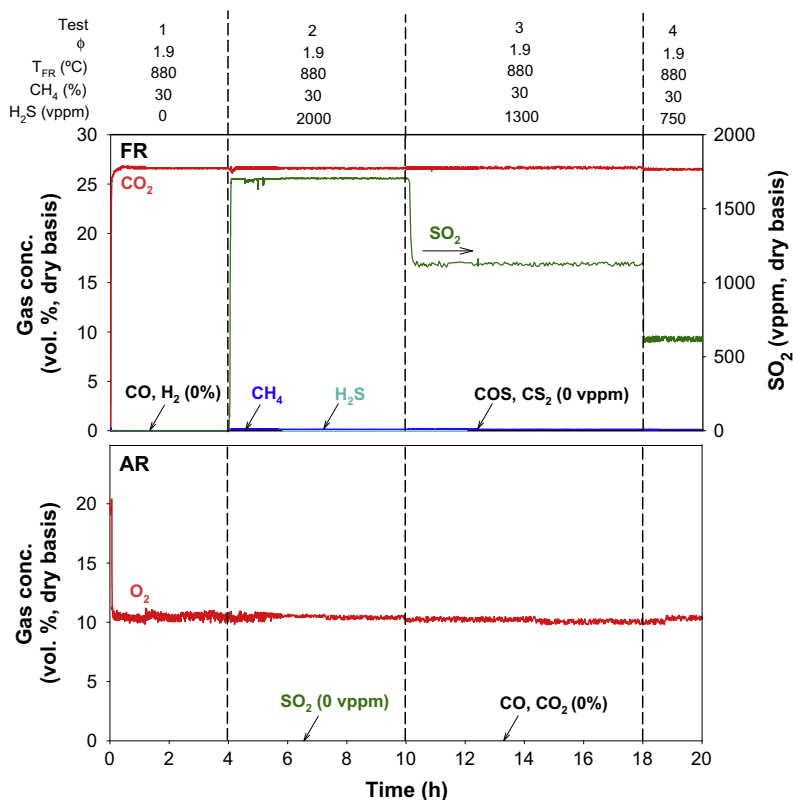


Fig. 3. Gas product distribution obtained at the outlet of AR and FR during different tests.

**Table 2**  
Mass balance of sulfur for each test.

	Test 2	Test 3	Test 4	Test 5	Test 6	Test 7	Test 8	Test 9
$\phi$	1.9	1.9	1.9	1.4	1.1	1.0	1.3	1.2
$H_2S$ fed (vppm)	2000	1300	750	1300	1300	1300	2000	2000
Sulfur distribution (%)								
In	100	100	100	100	100	100	100	100
Out gas FR	95.8	97.4	102.3	98.5	96.2	94.9	97.7	95.3
Out gas AR	0	0	0	0	0	0	0	0

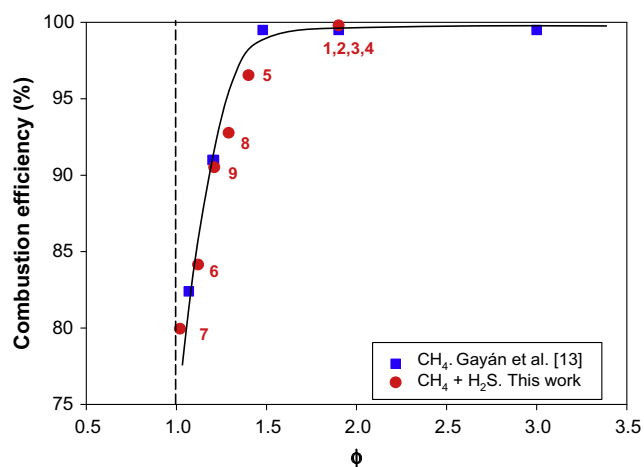


Fig. 4. Effect of the presence of  $H_2S$  in the fuel gas on the combustion efficiency for different oxygen carrier-to-fuel ratios,  $\phi$ . Numbers correspond to tests given in Table 1. For comparison reasons, tests carried out by Gayán et al. [13] have been added.

never showed agglomeration or defluidization problems in spite of the  $H_2S$  fed.

### 3.3.2. Oxygen carrier reducibility

Fresh and after-used samples were also analyzed by TPR technique in order to study the reducibility of the  $Fe_2O_3/Al_2O_3$  oxygen carrier. Fig. 5 illustrates the TPR profiles corresponding to the fresh sample and the samples extracted from the AR and FR of the CLC plant after tests 1 and 9. These tests correspond to the reference test without sulfur addition and the last test with  $H_2S$  addition in this experimental work, respectively. In this way, the effect of sulfur on the reducibility of the Fe-based oxygen carrier could be evaluated. The TPR profile corresponding to commercial pure  $Fe_2O_3$  particles was also included for comparison purposes.

The fresh sample exhibited three different hydrogen consumption peaks. The first peak at 683 K could be attributed to the reduction of isolated  $Fe_2O_3$  units on the surface of the support to  $Fe_3O_4$  with weak interaction with the support. The second peak at 985 K was attributed to the transition from  $Fe_3O_4$  to  $FeO$ . This reduction process took place at higher temperature than that for commercial  $Fe_2O_3$  (see Table 3), suggesting that the alumina had

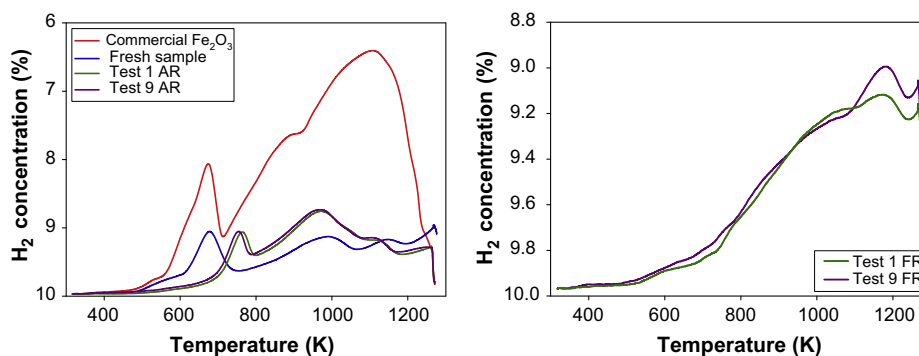


Fig. 5. TPR profiles of commercial  $\text{Fe}_2\text{O}_3$  and  $\text{Fe}_2\text{O}_3/\text{Al}_2\text{O}_3$  oxygen carrier particles, fresh and used particles extracted from the AR (left) and FR (right).

a stabilizing effect on the FeO metastable phase formed during reduction. Finally, the third peak corresponding to the last reduction step, the transition from FeO to  $\text{Fe}^0$ , took place at 1132 K. This third peak could not be attributed to the spinel formation ( $\text{FeO} \cdot \text{Al}_2\text{O}_3$ ) because the reduction temperature was not as high as necessary to reduce the spinel.

The samples extracted from the AR and FR in tests 1 and 9 showed very similar TPR patterns which indicated that the reducibility of the material was not affected by the presence of sulfur in the feeding gas. Regarding the samples taken from the AR, the first  $\text{H}_2$  consumption peak had a lower area than the one which corresponded to the reduction process from  $\text{Fe}_2\text{O}_3$  to  $\text{Fe}_3\text{O}_4$ . Furthermore, this peak was shifted to a higher temperature (760 K approximately) than that corresponding to the fresh sample, indicating that the interaction between the iron phases and the support was higher as the number of reduction–oxidation cycles in the continuous CLC unit was increased. The intensity of the second peak ( $\sim 970$  K) was higher than the one that corresponded to the fresh sample. Nevertheless, the intensity of the third step of reduction (a shoulder for both AR samples) was lower. This result could be explained in terms of that the reduction process  $\text{Fe}_3\text{O}_4 \rightarrow \text{FeO} \rightarrow \text{Fe}$  took place continuously, as it has been reported elsewhere [27].

In the samples taken from the FR it was observed a continuous  $\text{H}_2$  consumption up to a temperature close to 1173 K, when a small peak-shoulder could be found. This TPR profile could be indicative of the presence of different Fe phases in the samples. Thus, the reduction of  $\text{Fe}_2\text{O}_3$  to  $\text{Fe}_3\text{O}_4$  was combined with the presence of  $\text{Fe}_3\text{O}_4$  and iron aluminate ( $\text{FeO} \cdot \text{Al}_2\text{O}_3$ ) on the samples. This continuous reduction process can be found described by Ren-Yuan et al. [28]. Finally, the peak-shoulder that appeared at a higher temperature (around 1173 K) could indicate the reduction of  $\text{FeO} \cdot \text{Al}_2\text{O}_3$  to elemental Fe. The iron aluminate compound was only measured from TPR analysis carried out to FR-samples, as in TPR results of fresh and samples collected from the AR was not measured. Thus, it can be concluded that the iron aluminate was formed during the CLC reduction process in the FR. This result confirmed experimentally, as in the work conducted by Gayán et al. [13], that the presence of alumina in the oxygen carrier particles allowed the

reduction of the  $\text{Fe}_2\text{O}_3$  up to  $\text{Fe}^{+2}$ , in the form of  $\text{FeO} \cdot \text{Al}_2\text{O}_3$ , obtaining complete conversion of the gaseous fuel to  $\text{CO}_2$  and  $\text{H}_2\text{O}$  when the oxygen carrier-to-fuel ratio was high enough ( $\phi \geq 1.5$ ). Furthermore, the presence of iron aluminate in the samples extracted from the FR after each experimental test was also determined by X-ray Diffraction (XRD) analyses. In order to avoid the oxidation of these samples, the oxygen carrier particles were cooled in  $\text{N}_2$  to room temperature previously to be tested. Fig. 7 shows the powder XRD patterns of fresh and used particles extracted after 75 h of operation both from FR and AR.

### 3.3.3. Oxygen carrier reactivity

Fig. 6 shows the conversion vs time curves obtained both for the fresh material and the samples extracted from the CLC plant after tests 2 and 9. The data correspond to the third cycle of reduction–oxidation in the TGA. These three samples exhibited very similar reactivity both for reduction and oxidation, corroborating that the oxygen carrier reactivity was hardly affected by the presence of sulfur in the fuel gas.

### 3.3.4. Oxygen carrier structure

Sulfur mass balances for each experimental test closed in a range of  $\pm 5$  wt.%. The objective in this section is to verify, by means of different characterization techniques, the presence, or not, of sulfur in the oxygen carrier particles extracted from the CLC unit

Table 3  
Position of peaks for TPR analyses.

Sample	$T$ (K) reduction		
Commercial $\text{Fe}_2\text{O}_3$	673	898	1106
Fresh sample	683	985	1132
Test 1 AR	753	969	1105
Test 1 FR	Continuous $\text{H}_2$ consumption		
Test 9 AR	762	971	1105
Test 9 FR	Continuous $\text{H}_2$ consumption		

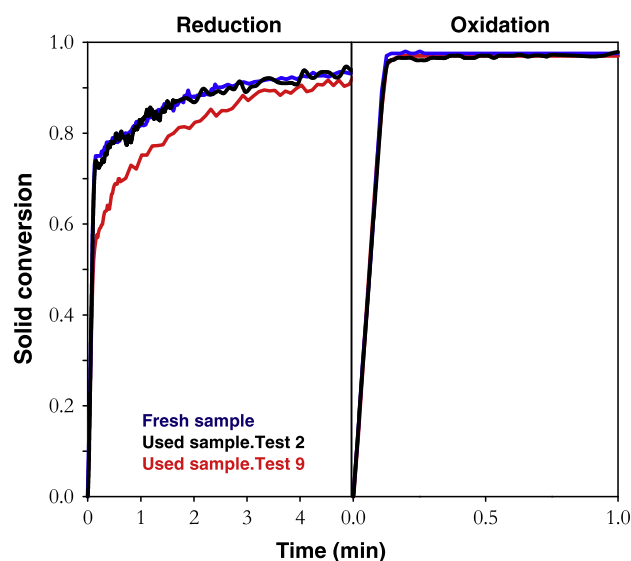


Fig. 6. TGA reactivity of fresh and after used particles. Reducing gas composition: 15 vol.%  $\text{CH}_4$ , 20 vol.%  $\text{H}_2\text{O}$  and  $\text{N}_2$  to balance. Oxidizing gas composition: pure air.  $T = 1223$  K.

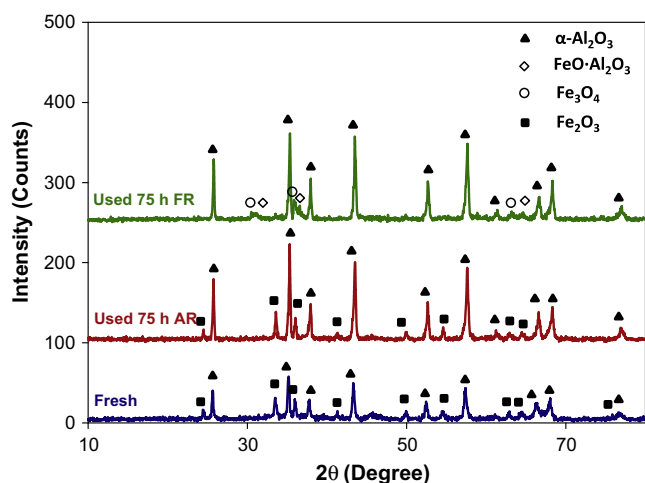


Fig. 7. XRD patterns of fresh and used particles extracted both from FR and AR after 75 h of operation.

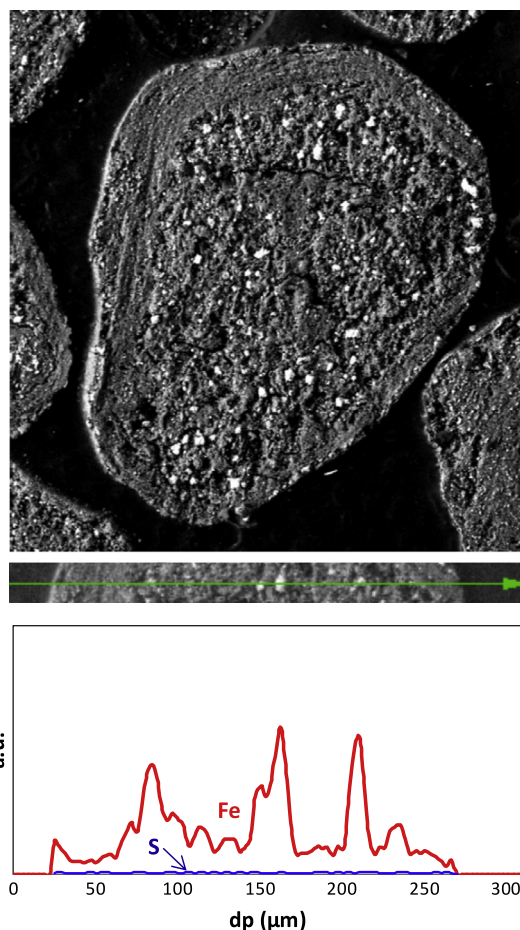


Fig. 8. SEM-EDX image of a cross-section of oxygen carrier particle after 75 h of operation in the CLC unit.

after the experimental tests with  $\text{H}_2\text{S}$  addition. These analyses would confirm that those minor differences in the closure of the sulfur balances were due to experimental errors.

From the powder XRD patterns it was concluded that there was no detection of any crystalline phase that contained sulfur in the structure of the particles, both extracted from the AR and the FR in any experimental test (see Fig. 7). However, it is important to

take into account that crystalline phases present in the samples with a mass percentage lower than 5 wt.% cannot be detected by means of XRD technique.

Oxygen carrier particles were also analyzed by SEM-EDX in order to check if sulfur was formed in the  $\text{Fe}_2\text{O}_3/\text{Al}_2\text{O}_3$  oxygen carrier during tests with sulfur addition. Fig. 8 illustrates a SEM image of a cross-section of oxygen carrier particle after 75 h of operation inside the CLC prototype. It can be stated that sulfur was not detected in the particles, neither inside nor in the external surface.

The characterization of this Fe-based material confirmed that no sulfur was detected in any of the used samples indicating that the small deviations in the sulfur mass balances showed in Table 2 can be attributed to experimental errors. Therefore, the oxygen carrier was capable of burning all the  $\text{H}_2\text{S}$  to  $\text{SO}_2$  without the formation of iron sulfides.

#### 4. Conclusions

A synthetic Fe-based oxygen carrier prepared by impregnation using  $\gamma\text{-Al}_2\text{O}_3$  as support was evaluated with respect to gas combustion in a 500  $\text{W}_{\text{th}}$  CLC continuous unit when the fuel,  $\text{CH}_4$ , contained variable amounts of  $\text{H}_2\text{S}$  (up to 2000 ppm).

The presence of  $\text{H}_2\text{S}$  in the fuel gas hardly affected the reactivity of the oxygen carrier and the combustion efficiency of the fuel gas, independently of the amount of sulfur present in the fuel stream. Full gas combustion conditions were achieved at  $\phi > 1.5$  operating at temperatures of 1173 K and 1223 K in the FR and AR respectively. In addition, all the sulfur fed with the fuel gas was released as  $\text{SO}_2$  in the flue gas from the FR. No sulfur was detected in the used samples extracted from the CLC unit after an exhaustive characterization of the oxygen carrier particles.

Some environmental considerations regarding sulfur presence in the different outlet streams of an industrial CLC unit that operated with this Fe-based oxygen can be drawn. Firstly, as the  $\text{SO}_2$  emissions released from the AR were non-existent, there would be no difficulty to fulfill the legislation about gaseous emissions in power plants. On the other hand, all the sulfur fed into the system was released as  $\text{SO}_2$  in the flue gas from the FR. This could mean important consequences with respect to the quality of the  $\text{CO}_2$  ready for sequestration that should be taken into account. The necessity of treatment of the flue gas downstream the FR would depend on the purity requirements of the liquefied  $\text{CO}_2$  to be transported, compressed and stored. Currently, there is no legislation about restrictive contaminant contents in  $\text{CO}_2$  for transport and storage, and much uncertainty exists about these limits [17].

On the basis of the experimental results obtained in this work, it can be concluded that the  $\text{Fe}_2\text{O}_3/\text{Al}_2\text{O}_3$  oxygen carrier presents an optimal behavior for the combustion of methane with hydrogen sulfide in the CLC prototype since this oxygen carrier was no susceptible to be poisoned by sulfur showing a very good reactivity and combustion efficiency when the fuel contained variable amounts of  $\text{H}_2\text{S}$ .

#### Acknowledgements

This paper is based on the work performed in the frame of the INNOCUOUS (Innovative Oxygen Carriers Uplifting Chemical – Looping Combustion) Project, funded by the European Commission under the seventh Framework Programme (Contract 241401). P. Gayán thanks to CSIC for the financial support of the project 201180E102.

#### References

- [1] Ishida M, Zheng D, Akehata T. Evaluation of a chemical-looping combustion power-generation system by graphic exergy analysis. *Energy* 1987;12:145–54.



- [2] Adánez J, Abad A, García-Labiano F, Gayán P, de Diego LF. Progress in chemical looping combustion and reforming technologies. *Prog Energy Combust Sci* 2012;38:215–82.
- [3] Jerndal E, Mattisson T, Lyngfelt A. Thermal analysis of chemical-looping combustion. *Chem Eng Res Des* 2006;84:795–806.
- [4] Leion H, Lyngfelt A, Johansson M, Jerndal E, Mattisson T. The use of ilmenite as an oxygen carrier in chemical-looping combustion. *Chem Eng Res Des* 2008;86:1017–26.
- [5] Abad A, García-Labiano F, de Diego LF, Gayán P, Adánez J. Reduction kinetics of Cu-, Ni- and Fe-based oxygen carriers using syngas ( $\text{CO} + \text{H}_2$ ) for chemical looping combustion. *Energy Fuel* 2007;21:1843–53.
- [6] Lyngfelt A, Thunman H. Construction and 100 h of operational experience of a 10-kW chemical-looping combustor. In: Thomas DC, Benson SM, editors. Carbon dioxide capture for storage in deep geologic formations—results from the  $\text{CO}_2$  capture project, vol. 1. Oxford, UK: Elsevier; 2005 [chapter 36].
- [7] Son SR, Kim SD. Chemical-looping combustion with  $\text{NiO}$  and  $\text{Fe}_2\text{O}_3$  in a thermobalance and circulating fluidized bed reactor with double loops. *Ind Eng Chem Res* 2006;45:2689–96.
- [8] Mattisson T, García-Labiano F, Kronberger B, Lyngfelt A, Adánez J, Hofbauer H. Chemical-looping combustion using syngas as fuel. *Int J Greenhouse Gas Control* 2007;1:158–69.
- [9] Abad A, Mattisson T, Lyngfelt A, Johansson M. The use of iron oxide as oxygen carrier in a chemical-looping reactor. *Fuel* 2007;86:1021–35.
- [10] Ortiz M, de Diego LF, Gayán P, Pans MA, García-Labiano F, Abad A, et al. Hydrogen production coupled with  $\text{CO}_2$  capture by chemical-looping using mixed Fe–Ni oxygen carriers. In: Proc 1st int conf on chemical looping. Lyon, France; 2010.
- [11] Ortiz M, Gayán P, de Diego LF, García-Labiano F, Abad A, Pans MA, et al. Hydrogen production with  $\text{CO}_2$  capture by coupling steam reforming of methane and chemical-looping combustion: use of an iron based waste product as oxygen carrier burning a PSA tail gas. *J Power Sour* 2011;196:4370–81.
- [12] Moldenhauer P, Ryden M, Lyngfelt A. Testing of minerals and industrial by-products as oxygen carriers for chemical-looping combustion in a circulating fluidized-bed 300 W laboratory reactor. *Fuel* 2012;93:351–63.
- [13] Gayán P, Pans MA, Ortiz M, Abad A, de Diego LF, García-Labiano F, et al. Testing of a highly reactive impregnated  $\text{Fe}_2\text{O}_3/\text{Al}_2\text{O}_3$  oxygen carrier for a SR-CLC system in a continuous CLC unit. *Fuel Process Technol* 2012;96:37–47.
- [14] Buckner D, Holmberg D, Griffin T. Techno-economic evaluation of an oxyfuel power plant using mixed conducting membranes. In: Thomas D, Benson S, editors. Carbon dioxide capture for storage in deep geologic formations. Results from the  $\text{CO}_2$  capture project, vol. 1. Oxford, UK: Elsevier Ltd.; 2005 [chapter 31].
- [15] Hebden D, Strout HJF. Coal gasification processes. In: Elliot MA, editor. Chemistry of coal utilization. New York: Wiley & Sons; 1981 [chapter 24].
- [16] Sass B, Monzyk B, Ricci S, Gupta A, Hindin B, Gupta N. Impact of  $\text{SO}_x$  and  $\text{NO}_x$  in flue gas on  $\text{CO}_2$  separation, compression, and pipeline transmission. In: Thomas DC, Benson SM, editors. Carbon dioxide capture for storage in deep geologic formations e results from the  $\text{CO}_2$  capture project, vol. 2. Oxford, UK: Elsevier; 2005 [chapter 17].
- [17] Bryant S, Lake LW. Effect of impurities on subsurface  $\text{CO}_2$  storage processes. In: Thomas DC, Benson SM, editors. Carbon dioxide capture for storage in deep geologic formations e results from the  $\text{CO}_2$  capture project, vol. 2. Oxford, UK: Elsevier; 2005 [chapter 18].
- [18] Wang B, Yan R, Lee DH, Liang DT, Zheng Y, Zhao H, et al. Thermodynamic investigation of carbon deposition and sulphur evolution in chemical looping combustion with syngas. *Energy Fuels* 2005;22:1012–20.
- [19] García-Labiano F, de Diego LF, Gayán P, Adánez J, Abad A, Dueso C. Effect of fuel gas composition in chemical-looping combustion with Ni-based oxygen carriers. 1. Fate of sulphur. *Ind Eng Chem Res* 2009;48:2499–508.
- [20] Forero CR, Gayán P, García-Labiano F, de Diego LF, Abad A, Adánez J. Effect of gas composition in chemical-looping combustion with copper-based oxygen carriers: fate of sulphur. *Int J Greenhouse Gas Control* 2010;4:762–70.
- [21] ASTM D5757-95: standard test method for determination of attrition and abrasion of powdered catalysts by air jets; ASTM: Philadelphia, PA; 1995.
- [22] Adánez J, de Diego LF, García-Labiano F, Gayán P, Abad A. Selection of oxygen carriers for chemical-looping combustion. *Energy Fuels* 2004;18:371–7.
- [23] HSC Chemistry 6.1, Chemical reaction and equilibrium software with thermochemical database and simulation module; Outotec Research Oy, Pori, Finland; 2008.
- [24] Adánez J, Dueso C, de Diego LF, García-Labiano F, Gayán P, Abad A. Methane combustion in a 500 W<sub>th</sub> chemical-looping combustion system using an impregnated Ni-based oxygen carrier. *Energy Fuels* 2009;23:130–42.
- [25] Forero CR, Gayán P, García-Labiano F, de Diego LF, Abad A, Adánez J. High temperature behaviour of a  $\text{CuO}/\text{Al}_2\text{O}_3$  oxygen carrier for chemical-looping combustion. *Int J Greenhouse Gas Control* 2011;5:659–67.
- [26] Gupta RP, Turk BS, Vierheilig AA. Desulfurization sorbents for transport-bed applications. In: Proceedings of the advanced coal-based and environmental systems. Pittsburgh, USA; 1997.
- [27] Park JY, Lee YJ, Khanna PK, Jun KW, Bae JW, Kim YH. Alumina-supported iron oxide nanoparticles as Fisher–Tropsch catalysts: effect of particle size of iron oxide. *J Mol Catal A: Chem* 2010;323:84–90.
- [28] Ren-Yuan T, Su Z, Chengu W, Dongbai L, Liwu L. An in situ combined temperature-programmed reduction–Mössbauer spectroscopy of alumina-supported iron catalysts. *J Catal* 1987;106:440–8.